


Article

Regular and Irregular Performance Variation of Module String and Occurred Conditions for Potential Induced Degradation-Affected Crystalline Silicon Photovoltaic Power Plants

Jingsheng Huang ^{1,2}, Yaojie Sun ^{1,*}, He Wang ^{3,*}  and Junjun Zhang ⁴

¹ School of Information Science and Technology, Fudan University, Shanghai 200433, China; huangjingsheng@jsyhkf.com

² Jiangsu Coast Development Investment Co., Ltd., Nanjing 210000, China

³ MOE Key Laboratory for Nonequilibrium Synthesis and Modulation of Condensed Matter, School of Science, Xi'an Jiaotong University, Xi'an 710049, China

⁴ State Key Laboratory of Operation and Control of Renewable Energy & Storage Systems, China Electric Power Research Institute, Nanjing 210003, China; zhangjunjun@epri.sgcc.com.cn

* Correspondence: yjsun@fudan.edu.cn (Y.S.); hw69cn@126.com (H.W.)

Received: 12 October 2019; Accepted: 3 November 2019; Published: 6 November 2019



Abstract: Potential induced degradation (PID) leads to power degradation, and reduces durability and reliability of solar modules. However, this problem has not been thoroughly solved so far. The results from interlaboratory and field study show contradictory fault phenomenon for PID. In this paper, PID of crystalline silicon photovoltaic power plants distributed in various climate conditions was investigated. These photovoltaic power plants consist of two types of crystalline silicon solar modules, which cover almost all kinds of front glass, ethyl vinyl acetate (EVA) and backsheets available commercially. It was found that only a few of power plants were affected by PID. By measuring current voltage characteristics of PID-affected solar modules, the real faults phenomenon was uncovered and classified into regular and irregular power degradation in a module string. The results obtained in this work show that the negative potential caused by high system voltage and stacking faults are necessary and sufficient conditions for PID occurrence for the first time. The anomalous power degradation is related to the stacking fault, which appears randomly during the crystal growth.

Keywords: solar module; power degradation; crystalline silicon; potential induced degradation

1. Introduction

Crystalline silicon solar modules have a high reliability and low total number of returns, this is found in the peak power warranty clause supplied by the module producers, which are currently as high as 25 years [1–5]. However, the potential induced degradation caused a remarkable degradation of output power for photovoltaic power plant in recent years [6–8]. This has a bad influence on performance ratio and rate of return on investment for photovoltaic power plant. Since Swanson reported significant power loss for SunPower's back-contacted n-type solar modules in the field due to PID, many researchers have devoted their time to solving this problem at solar cells, modules, and systems level [9–14]. V. Naumann et al. think that PID is related with sodium decorated stacking faults across the pn junction under high system voltage [15–18]. S. Koch, K. Mishina and Zhou found that adding two or three layers coatings into crystalline silicon solar cells could reduce the sensitivity of PID [19–21]. J. Hylsky et al. deem that crystalline silicon solar cells with the phosphorus silicate glass

show properties resistive against PID [22]. J. Kapur and A. Virtuani believe that the encapsulation materials could directly affect the extent of PID [23,24]. S. Hoffmann et al. think that PID could be accelerated by environmental factors such as temperature and humidity [25]. S. Suzuki et al. confirmed that PID in crystalline silicon photovoltaic modules could be accelerated by salt-mist preconditioning [26]. At the photovoltaic system level, some researchers think that the applied negative voltage could remove the sodium ions embedded in the stacking faults, and regain the output power of PID-affected crystalline silicon solar modules [27–30]. But up to now, the true cause and occurred conditions of PID have not been found thoroughly yet because of complication of PID phenomena. People have not found the sufficient and necessary conditions for PID. In this paper, by investigating the crystalline silicon photovoltaic power plants in various climate conditions, we found that only a few of power plant suffered from PID. These results prove that the potential between crystalline silicon solar cells and the aluminium frame is necessary but is not a sufficient condition for occurrence of PID. The measured photovoltaic power plants consist of two crystalline silicon solar module types, which cover almost all kinds of front glass, EVA and backsheet available commercially. We found that PID is not directly relevant to encapsulation materials. Some proper encapsulation materials of solar modules could only slow PID down. By measuring electrical performance of PID-affected solar modules, the real faults phenomenon were revealed and classified into regular and irregular power degradation in a module string. It was found that the deterioration degree of PID-affected solar modules is not proportional to the applied voltage between solar cells and aluminum frame in some cases in the field, this result agrees with [31]. These findings are a little different from previous study [32]. We think that the anomalous power degradation is related to the stacking fault which appears randomly during the crystal growth. The negative potential and stacking faults are necessary and sufficient conditions for PID occurrence.

2. Materials and Methods

The crystalline silicon photovoltaic power plants studied in this work are distributed in various climate conditions in China. These photovoltaic power plants consist of two crystalline silicon solar module types, i.e., monocrystalline silicon (Mono-Si) solar modules and multicrystalline silicon (Multi-Si) solar modules. The solar modules used in these power plants consist of 60- or 72- piece p-type Mono-Si or Multi-Si solar cells wired in series, respectively. These crystalline silicon solar cells were encapsulated with the classic glass-EVA-cells-EVA-backsheet structure, which cover almost all kinds of front glass, EVA and backsheet available commercially. For every solar module, three bypass diodes were placed in junction box. Also, 20 or 24 crystalline silicon solar cells were serially connected with a bypass diode. The dimensions of crystalline silicon solar cells are $125 \times 125 \text{ mm}^2$ or $156 \times 156 \text{ mm}^2$, and have a conventional H-pattern model and an unpassivated full-area screen-printed aluminium back surface field.

Figure 1 gives out the studied photovoltaic power plants and experimental setup. 20~25°C environmental temperature, 820~900 W/m² solar irradiance and 1–2 m/s wind speed were chosen as test conditions in the field. The current-voltage characteristics and output power-voltage characteristics of solar modules were tested by the portable XJTU-10A in the field. The voltages of module strings under open circuit (V_{oc}) were tested by portable digital multimeter (Fluke Corp., Fluke 15B+). Thermography images (IR images) of crystalline silicon solar modules were acquired by T420 (FLIR Systems, Inc. USA) with a resolution of 320×240 pixels. The spectral range of T420 is 7.5~13µm. And solar modules suffered from PID can be distinguished by its open circuit voltage and the thermography image [14]. The intensity of sunlight was tested by YFJ-10 solar irradiation meter. The working temperature of solar module was tested by thermocouple. The solar modules suffered from PID were labelled in sequence respectively and disassembled from module string, and carried to our laboratory. The current-voltage characteristics of PID-affected solar modules disassembled from photovoltaic array was measured by solar simulator (PASAN Sunsim 3C) under standard test conditions (STC: 1 kW/m² irradiation, 25°C module temperature and AM1.5 global spectrum). The solar

simulator was adjusted by the same type standard module. The electroluminescence images (EL images) of the crystalline silicon solar modules were tested by an EL measurement system indoor.



Figure 1. The studied photovoltaic power plants and experimental setup.

3. Results

3.1. Probability of PID for Crystalline Silicon Photovoltaic Power Plants Distributed in Various Climate Conditions

In order to find out the reasons for occurrence of PID, the crystalline silicon photovoltaic power plants located in different climate zones were tested. Figure 2 gives out the distribution of the tested photovoltaic power plants. These photovoltaic power plants range from hot to cold and humid to arid.

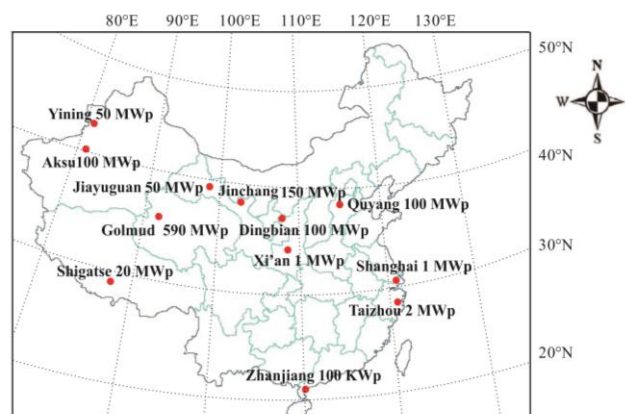


Figure 2. The distribution of photovoltaic power plant at different climate regions.

Figure 3 shows the typical electrical topology of sub-array for the photovoltaic power stations. In Figure 3, 16~18 or 20~22 crystalline silicon solar modules were concatenated into module string. A string box with direct current switch was used to connect the module strings in parallel. The string

box was directly concatenated to solar inverter. The Al frame of solar module was grounded for the sake of preventing electric shock.

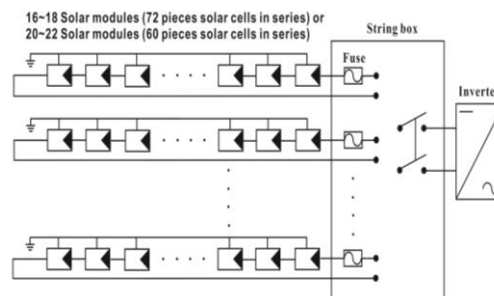


Figure 3. Typical electrical topology of sub-array for the studied photovoltaic power stations. 16~18 or 20~22 crystalline silicon solar modules were concatenated into module string. A string box with direct current switch was used to connect the module strings in parallel. The string box was directly concatenated to solar inverter. The aluminium frame of solar module was grounded for the sake of preventing electric shock.

Table 1 gives out the information of the studied power plants, and a certain power plant is or not affected by PID. From Table 1, it was found that only multicrystalline silicon solar modules in Quyang, monocrystalline silicon solar modules in Dingbian and Zhanjiang suffered from PID. The probability of PID for multicrystalline silicon photovoltaic power plants is 6.28%, and the probability of PID for monocrystalline silicon photovoltaic power plants is 6.81%. In these power plants, some solar modules exposed to negative potential show an abnormal power degradation caused by PID, but other solar modules exposed to negative potential are PID-free. So this result confirms that negative potential is necessary condition for PID, and negative potential is not sufficient condition for PID. Some of findings agree with many published papers [33–35].

Table 1. Summary of the studied photovoltaic power plants.

| Location | Latitude (N) | Longitude (E) | Installed Capacity (MW _p) | Module Technology | PID or PID-Free |
|-----------|--------------|---------------|---------------------------------------|-------------------|-----------------|
| Yining | 44°01′ | 81°17′ | 50 | Multi-Si | PID-free |
| Aksu | 40°21′ | 81°09′ | 100 | Multi-Si | PID-free |
| Jiayuguan | 39°48′ | 98°17′ | 50 | Multi-Si | PID-free |
| Quyang | 38°42′ | 114°40′ | 100 | Multi-Si | PID |
| Jinchang | 38°31′ | 102°12′ | 150 | Multi-Si | PID-free |
| Golmud | 35°35′ | 92°42′ | 590 | Multi-Si& Mono-Si | PID-free |
| Dingbian | 37°23′ | 107°45′ | 100 | Multi-Si& Mono-Si | PID (Mono-Si) |
| Xi'an | 34°17′ | 108°57′ | 1 | Multi-Si | PID-free |
| Shanghai | 31°15′ | 121°29′ | 1 | Multi-Si& Mono-Si | PID-free |
| Shigatse | 29°16′ | 88°57′ | 20 | Mono-Si | PID-free |
| Taizhou | 28°40′ | 121°26′ | 2 | Mono-Si | PID-free |
| Zhanjiang | 21°15′ | 110°22′ | 0.1 | Mono-Si | PID |

Quyang and Dingbian have a moderate climate, and Zhanjiang has a hot and humid climate. According to Table 1, the photovoltaic power plants located in Quyang and Dingbian suffered from PID, so high temperature and humid are not the necessary prerequisite to occurrence of PID, but the high temperature and humid could aggravate the extent of PID [10].

In these power plants, the solar modules used almost all of the front glass, EVA and backsheet available commercially. It was also not found that occurrence of PID is related with EVA, backsheet, monocrystalline or multicrystalline silicon solar cells from Table 1.

3.2. Regular and Irregular Performance Deterioration of Module Strings from PID-Affected Power Plants

3.2.1. Regular and Irregular Degradation of Open Circuit Voltage of Module Strings under Field Conditions

Figure 4 shows the potential distribution of crystalline silicon solar module between solar cells and an aluminium frame for two types of module strings. Figure 4a shows the potential of module string made up of 17 solar modules with 72 pieces solar cells in series, Figure 4b gives out the potential of module string made up of 22 solar modules with 60 pieces solar cells in series. The potential of the aluminium frame is zero because it is grounded. For crystalline silicon solar modules situated on the front half module string, the potential of solar cells is positive relative to aluminium frame. For solar modules located in the rear half module string, the potential of solar cells is negative relative to the aluminium frame. The potential is caused by high voltage formed by the series connection of solar modules. The potential that each solar module sustains is directly proportional to the serial number of the modules in working conditions [36]. For a certain PID-affected power plant, the encapsulated materials of all solar modules are the same, and the working conditions, such as illumination, temperature, relative humidity, soil, rain, and etc. are also the same except the potential that solar module endures. If the viewpoint of surface polarization effect for PID mechanism is correct, out of question, the degradation rate of power is relevant to the location of each module in module string, i.e., the closer the solar module approaches the negative pole of module string, the more serious the deterioration of maximum power for the solar module is. If the standpoint of sodium-decorated stacking faults across n^+ -p junctions for PID mechanism is correct, the deterioration degree of solar module will increase with the increasing of module sequence number only when the density of stacking faults on all solar cells in a certain module string is nearly equal.

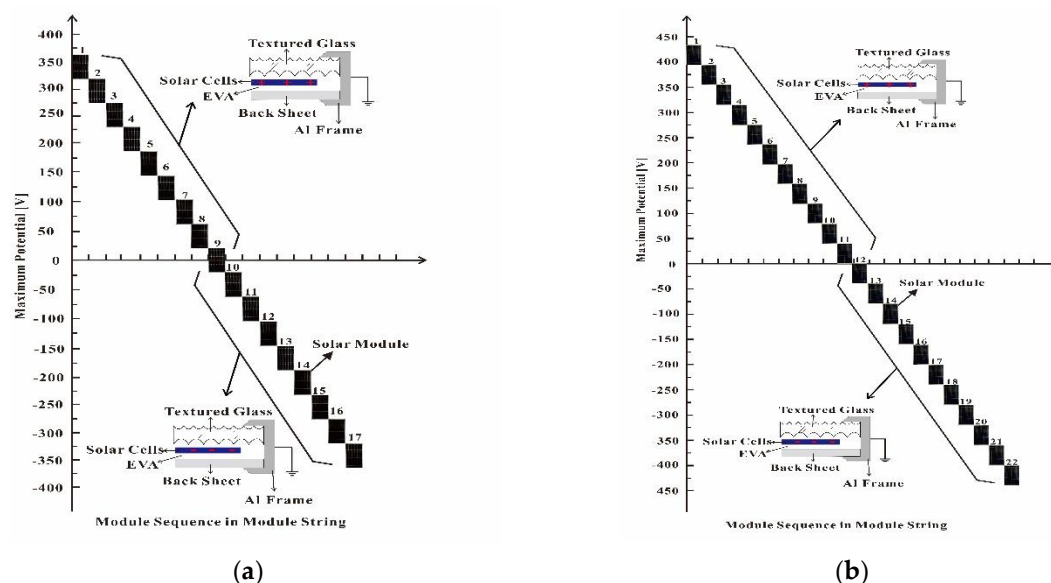


Figure 4. The potential distribution of solar modules between solar cell and aluminium frame in two types of module string. (a) Module string made up of 17 solar modules with 72 pieces solar cells in series; (b) Module string made up of 22 solar modules with 60 pieces solar cells in series.

The relationship between open circuit voltages of crystalline silicon solar modules and module sequence in PID-affected solar module strings corresponding to Figure 4 respectively for the two PID-affected power plants is shown in Figure 5. In Figure 5, the open circuit voltages of solar modules were measured in the field and translated to STC by XJTU-10A.

From Figure 5a, it was found that the open circuit voltages of crystalline silicon solar modules from module 1 to module 9 are almost equal for all monocrystalline silicon module strings, and there is

almost no degradation. But the open circuit voltages of modules from module 10 to module 17 decrease gradually with the increasing module number for the module string 1 to 5. This finding seems to give us some hints that there is a relationship between the extent of PID and the potential of solar modules in some cases. This result agrees with [32,37]. But for module string 6, 7 and 8, the voltages of solar modules from No. 10 to No. 17 under open circuit show an irregular change with the increasing module number, this result agrees with [31]. From Figure 5b, it could be seen that the voltages of solar modules from module 1 to module 11 under open circuit are nearly the same, and there is almost no degradation for open circuit voltages. But for the module 12 to module 22, the open circuit voltages show an irregular change with the increasing module number. This shows that the extent of PID is not proportional to the value of potential in such situation.

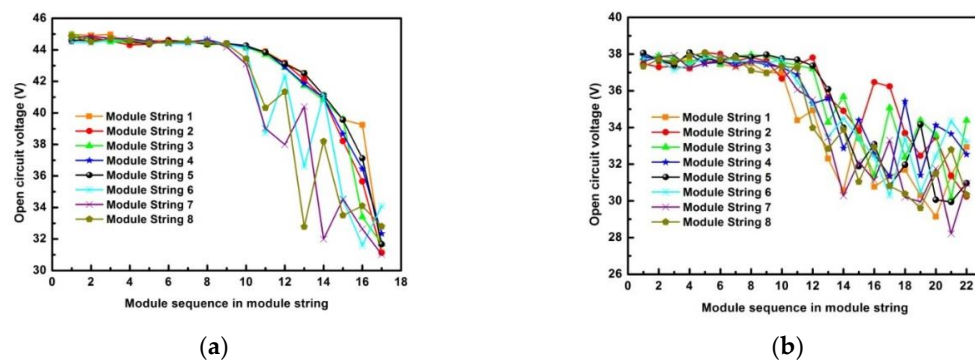


Figure 5. The relationship between the voltages of solar modules under open circuit and module sequence in PID-affected monocrystalline silicon module string (a) and multicrystalline silicon module string (b). The values of open circuit voltage were measured in the field and translated to STC.

3.2.2. Parametric Analysis of Solar Modules Dismounted from PID-Affected Power Plants under STC

The PID-affected monocrystalline and multicrystalline silicon solar modules from different power plants were labelled in order respectively and disassembled from module strings, and carried to lab for degradation investigation under STC. Figure 6 gives out the current-voltage and power-voltage curves of 17 monocrystalline silicon modules dismounted from the module string 1 corresponding to Figure 5a. From Figure 6, it was found that the maximum output powers of module 1 to 9 almost have no degradation. But the solar module 10 to 17 exhibit different degrees of power degradation with the increasing module number, even if these solar modules suffered from an even growth of potential with the increasing module number, i.e., it was not found that the larger negative potential induce more serious PID in proportion.

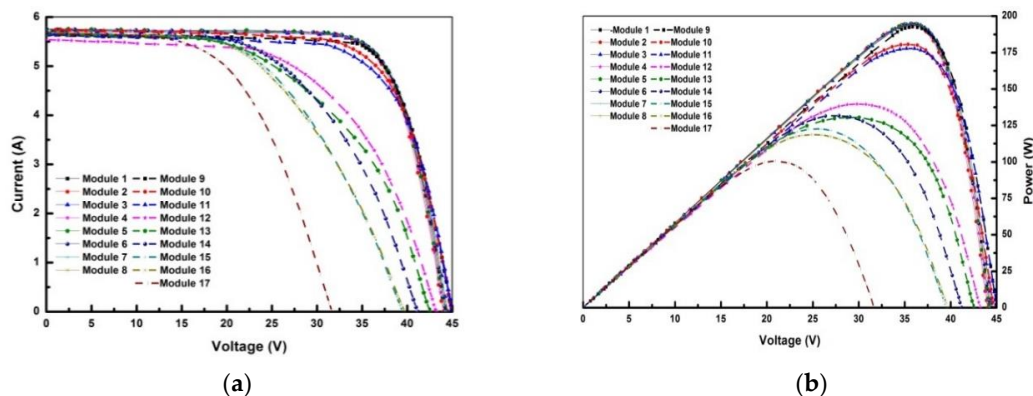


Figure 6. The current-voltage characteristics (a) and power-voltage characteristics (b) of 17 monocrystalline silicon solar modules dismounted from PID-affected module string 1. The larger negative potential did not induce more serious PID in proportion.

Figure 7 gives out the current-voltage characteristics and power-voltage characteristics of 17 monocrystalline silicon solar modules dismantled from the module string 7 corresponding to Figure 5a. From Figure 7, it was found that the electrical parameters of module 1 to 9 show a normal degradation caused by light-induced degradation. But the maximum output powers of module 10 to 17 show an irregular degradation with the increasing module number. The deterioration degree of Module 14 in Figure 7 is more serious than that of module 15 and module 16. This is different from that of Module string 1 of Figure 6. In other words, even if module 14 of module string 7 underwent a lower negative potential than that of module 15 and module 16 in the field, module 14 shows more power degradation than module 15 and module 16. Thus, it is proved that there is another important factor about the extent of PID in addition to this potential.

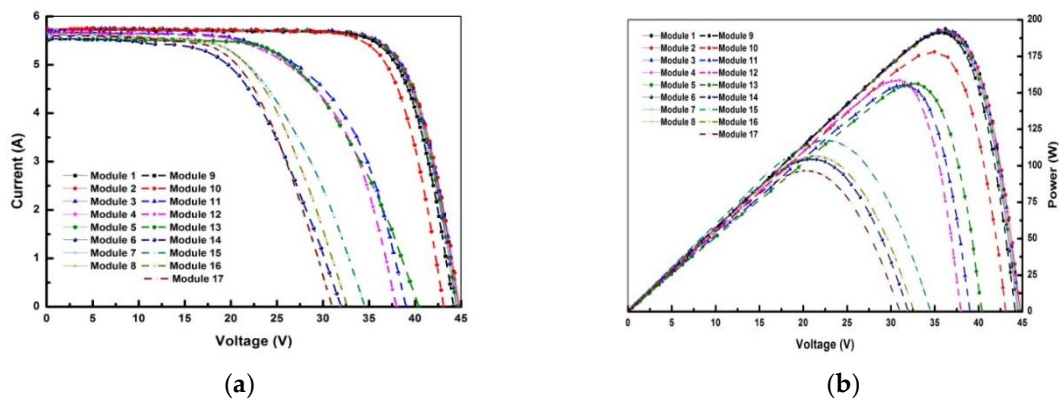


Figure 7. The current-voltage characteristics (a) and power-voltage characteristics (b) of 17 solar modules dismantled from PID-affected module string 7. Although solar module 14 undergone a lower negative potential than that of module 15 and module 16 in the field, module 14 shows a more power degradation than module 15 and module 16.

Figure 8 gives out the current-voltage characteristics and power-voltage characteristics of 22 multicrystalline silicon solar modules dismantled from module string 1 corresponding to Figure 5b. From Figure 8, it was found that the electrical parameters of module 1 to 11 show normal power degradation induced by the boron-oxygen complex. But the deterioration degrees of module 12 to 22 do not increase with the increasing module number. Module 20 in Figure 8 shows the largest performance deterioration with power degradation of 48% and open circuit voltage degradation of 23%, respectively.

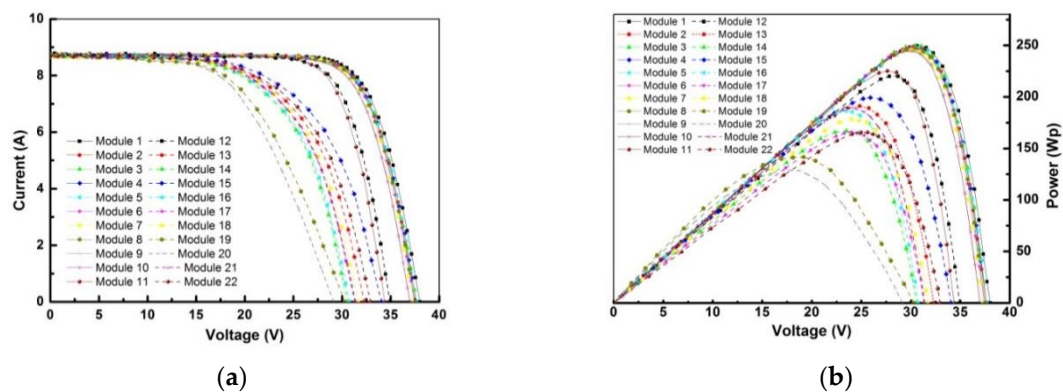


Figure 8. The current-voltage characteristics (a) and power-voltage characteristics (b) of 22 multicrystalline silicon solar modules dismantled from PID-affected module string 1. Solar module 20 shows the largest performance deterioration with power degradation of 48% and open circuit voltage degradation of 23%, respectively.

Figure 9 shows the change of maximum power of modules from 3 different PID-affected module strings, which are monocrystalline silicon module strings 1 and 7 of Figure 5a, and multicrystalline silicon module string 1 of Figure 5b, respectively. From Figure 9, it was found that the solar modules located in the front half-string shows a normal power degradation caused by light-induced degradation, and the deterioration degrees of solar modules located in the rear half-string do not increase with the increasing negative potential except for partial monocrystalline silicon module strings. From Figure 9 and Table 1, it was also found that the negative potential relative to the aluminium frame is not sufficient, but is a necessary condition for PID. The severity of PID is not necessarily related to the magnitude of negative potential in the field. But in laboratory, the higher applied negative voltage induces more severe PID for a certain PID-susceptible solar modules. The positive potential does not induce PID. This result agrees with [37].

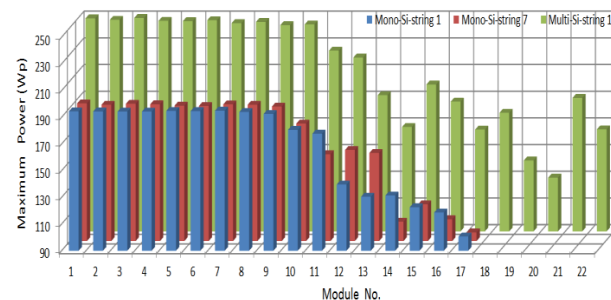


Figure 9. The change of the maximum output power for three module strings, which are monocrystalline silicon module string 1 and 7 of Figure 5a, and multicrystalline silicon module string 1 of Figure 5b, respectively.

3.2.3. Electroluminescence Images and Thermography Images for Monocrystalline and Multicrystalline Silicon Solar Modules Suffered from PID

In some cases, the electroluminescence images and thermography images of monocrystalline silicon solar modules from the same PID-affected module string present a regular change, as shown in Figure 10. From Figure 10, it was found that the solar cells near the aluminium frame exhibit higher temperatures than the middle solar cells in module 17; this has been proven by [36]. But in other cases, the EL image and IR image of PID-affected monocrystalline silicon solar module dismantled from the module string present an irregular change, as shown in Figure 11. From Figure 11, it was found that the solar cells near the aluminium frame do not exhibit high temperature than middle solar cells in module 14, even if the solar cells near to the aluminium frame sustain larger negative potential [32]. This finding is different from Figure 10.

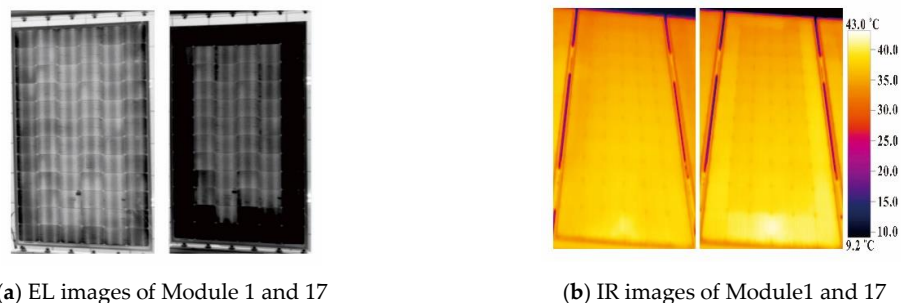


Figure 10. The electroluminescence images and thermography images of monocrystalline silicon solar modules from the same PID-affected module string. The left in (a) is electroluminescence image for module 1, the right in (a) is electroluminescence image for module 17. The left in (b) is thermography image for module 1, the right in (b) is thermography image for module 17. The solar cells near to the aluminium frame exhibit higher temperatures than the middle solar cells in module 17. Reprint from [33]. Copyright 2017, Elsevier.



Figure 11. The electroluminescence image (a) and thermography image (b) of module 14 from the module string 7 corresponding to Figure 5a. The EL image and IR image of PID-affected monocrystalline silicon solar module exhibit an irregular change.

Figure 12 gives out the typical EL image and IR image of PID-affected multicrystalline silicon solar module from the module string. From Figure 12, it was found that there is not a regular change in PID-affected multicrystalline silicon solar module, i.e., the solar cells adjacent to the aluminium frame do not exhibit higher temperature than the middle cells in the multicrystalline silicon solar module. According to the measured results from the field, we did not also find the regular change of IR images and EL images for PID-affected multicrystalline silicon module string in the photovoltaic power plants.

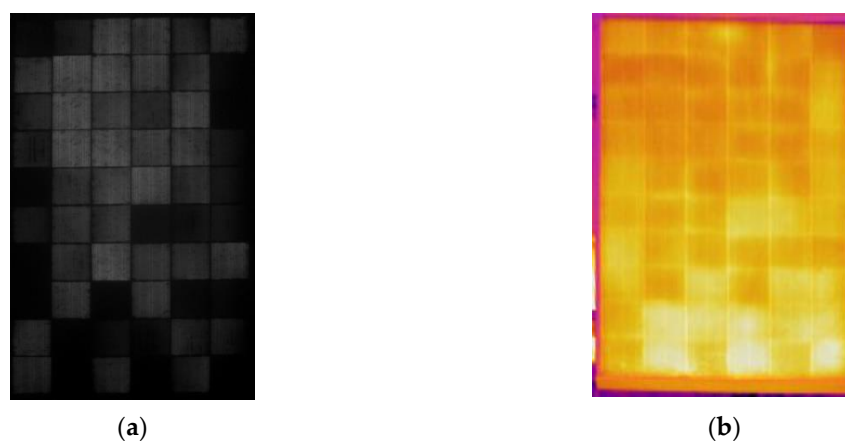


Figure 12. The typical electroluminescence image (a) and thermography image (b) of multicrystalline silicon solar module suffered from PID from the field.

The above results prove that there are regular and irregular electroluminescence images and thermography images of monocrystalline silicon modules that suffered from PID in the field, and it was not found that there are the regular electroluminescence images and thermography images of multicrystalline silicon solar modules that suffered from PID, as far as we know.

4. Discussion

According to the aforementioned results, the probability of PID for monocrystalline and multicrystalline silicon photovoltaic power plants is very small for the installed power plants in China. There are regular and irregular electroluminescence images and thermography images for monocrystalline silicon solar modules that suffered from PID in the field. It was not found that there were regular electroluminescence images and thermography images for multicrystalline silicon solar modules that suffered from PID. These results could be explained by preparation process of monocrystalline and multicrystalline silicon solar modules.

Usually, the monocrystalline silicon ingots are produced by Czochralski technology. In recent years, the length of silicon ingot has reached 3.5 m or so, and the growth speed of monocrystalline silicon ingot has been improved from 0.8 mm/min to 1.6 mm/min so as to reducing process costs. The stacking faults that emerged in semiconductor-grade silicon may go back to solar-grade silicon. Because the rate of rotation and pulling could be controlled accurately, the stacking faults may be formed uniformly. During subsequent automatic production, the similar monocrystalline silicon solar modules were installed in a module string. Thus, it is likely to present a regular degradation in monocrystalline silicon power plants. Multicrystalline silicon ingots are usually produced by a directional solidification technique; the length and width of multicrystalline silicon ingot are nearly 1 m, but the height of multicrystalline silicon ingot is only less than 0.4 m. Stacking faults is not likely well-distributed on bricks cut from a multicrystalline silicon ingot. Compared with monocrystalline silicon ingot, such a growth characteristic for multicrystalline silicon leads to a higher probability of irregular degradation in multicrystalline silicon power plants.

In summary, in terms of the outcome, we think the negative potential and stacking faults are necessary and sufficient conditions for PID occurrence [34,38–40]. Because sodium ions exist in every material of solar module besides rain and soil, some encapsulation materials with a low sodium ion concentration only alleviate PID of the solar module for a period of time. The high temperature and humidity are beneficial to migration of sodium ion, so the high temperature and humid could aggravate the extent of PID [41–45]. Because of the complication of stacking faults, it is nearly impossible to calculate power degradation as a function of negative system bias, stress time, module temperature and relative humidity.

5. Conclusions

In this paper, PID of crystalline silicon photovoltaic power plants distributed in various climate conditions was investigated. It was found that only a few power plants suffered from PID. In our study, the probability of PID for multicrystalline silicon photovoltaic power plants is 6.28%, and the probability of PID for monocrystalline silicon photovoltaic power plants is 6.81%. By measuring electrical characteristics of solar modules suffered from PID, the real faults phenomenon was revealed and classified into regular and irregular power degradation in the field for the first time. Owing to occasional stacking faults, it was found that there is no a general relationship between the degradation rate of open circuit voltage and applied negative potential for PID-affected solar modules, and there is also no a general relationship between the degradation rate of output power and applied negative potential for PID-affected solar modules. EL and IR images prove that there are regular and irregular electroluminescence images and thermography images for monocrystalline silicon solar modules suffered from PID in the field. It was not found that there were regular electroluminescence images and thermography images for multicrystalline silicon solar modules. These phenomena are explained by a preparation process of monocrystalline silicon and multicrystalline silicon solar modules. The analysis of the results underlines the fact that the negative potential and stacking faults are necessary and sufficient conditions for PID occurrence.

Author Contributions: Conceptualization, J.H. and H.W.; Methodology, Y.S.; Investigation, J.H.; writing—original draft preparation, J.H.; writing—review and editing, Y.S.; funding acquisition, H.W. and J.Z.

Funding: This research was funded by the National Key R&D Program of China, grant number 2018YFB1500700.

Conflicts of Interest: The authors declare no conflict of interest.

References

1. Osterwald, C.R.; McMahon, T.J. History of accelerated and qualification testing of terrestrial photovoltaic modules: A literature review. *Prog. Photovolt. Res. Appl.* **2009**, *17*, 11–33. [\[CrossRef\]](#)
2. Munoz, M.A.; Alonso-Garcia, M.C.; Vela, N.; Chenlo, F. Early degradation of silicon PV modules and guaranty conditions. *Sol. Energy* **2011**, *85*, 2264–2274. [\[CrossRef\]](#)

3. Ishii, T.; Takashima, T.; Otani, K. Long-term performance degradation of various kinds of photovoltaic modules under moderate climatic. *Prog. Photovolt. Res. Appl.* **2011**, *19*, 170–179. [[CrossRef](#)]
4. Kahoul, N.; Chenni, R.; Cheghib, H.; Mekhilef, S. Evaluating the reliability of crystalline silicon photovoltaic modules in harsh environment. *Renew. Energy* **2017**, *109*, 66–72. [[CrossRef](#)]
5. Schneller, E.J.; Brooker, R.P.; Shiradkar, N.S.; Rodgers, M.P.; Dhere, N.G.; Davis, K.O.; Seigneur, H.P.; Mohajeri, N.; Wohlgemuth, J.; Scardera, G.; et al. Manufacturing metrology for c-Si module reliability and durability Part III: Module manufacturing. *Renew. Sustain. Energy Rev.* **2016**, *59*, 992–1016. [[CrossRef](#)]
6. Luo, W.; Khoo, Y.S.; Hacke, P.; Naumann, V.; Lausch, D.; Harvey, S.P.; Singh, J.P.; Chai, J.; Wang, Y.; Aberle, A.G.; et al. Potential-induced degradation in photovoltaic modules: A critical review. *Energy Environ. Sci.* **2017**, *10*, 43–68. [[CrossRef](#)]
7. Yamaguchi, S.; Masuda, A.; Ohdaira, K. Changes in the current density-voltage and external quantum efficiency characteristics of n-type single-crystalline silicon photovoltaic modules with a rear-side emitter undergoing potential-induced degradation. *Sol. Energy Mater. Sol. Cells* **2016**, *151*, 113–119. [[CrossRef](#)]
8. Hacke, P.; Terwilliger, K.; Glick, S.; Tamizhmani, G.; Tatapudi, S.; Stark, C.; Koch, S.; Weber, T.; Berghold, J.; Hoffmann, S.; et al. Interlaboratory Study to Determine Repeatability of the Damp-Heat Test Method for Potential-Induced Degradation and Polarization in Crystalline Silicon Photovoltaic Modules. *IEEE J. Photovolt.* **2015**, *5*, 94–101. [[CrossRef](#)]
9. Swanson, R.; Cudzinovic, M.; Deceuster, D.; Desai, V.; Jurgens, J.; Kaminar, N.; Mulligan, W.; Rodrigues-Barbosa, L.; Rose, D.; Smith, D.; et al. The surface polarization effect in high efficiency silicon solar cells. In Proceedings of the 15th International Photovoltaic Science & Engineering Conference, Shanghai, China, 10–15 October 2005; pp. 410–413.
10. Hacke, P.; Smith, R.; Terwilliger, K.; Perrin, G.; Sekulic, B.; Kurtz, S. Development of an IEC test for crystalline silicon modules to qualify their resistance to system voltage stress. *Prog. Photovolt. Res. Appl.* **2014**, *22*, 775–783. [[CrossRef](#)]
11. Oh, J.; Bowden, S.; Tamizhmani, G. Potential-induced degradation (PID): Incomplete recovery of shunt resistance and quantum efficiency losses. *IEEE J. Photovolt.* **2015**, *6*, 1540–1548.
12. Koentopp, M.B.; Krober, M.; Taubitz, C. Toward a PID standard: Understanding and modeling of laboratory tests and field progression. *IEEE J. Photovolt.* **2016**, *6*, 252–257. [[CrossRef](#)]
13. Koehl, M.; Hoffmann, S. Impact of rain and soiling on potential induced degradation. *Prog. Photovolt. Res. Appl.* **2016**, *24*, 1304–1309. [[CrossRef](#)]
14. Kaden, T.; Lammers, K.; Moller, H.J. Power loss prognosis from thermographic images of PID affected silicon solar modules. *Sol. Energy Mater. Sol. Cells* **2015**, *142*, 24–28. [[CrossRef](#)]
15. Naumann, V.; Lausch, D.; Hahnel, A.; Bauer, J.; Breitenstein, O.; Graff, A.; Werner, M.; Swatek, S.; Großer, S.; Bagdahn, J.; et al. Explanation of potential-induced degradation of the shunting type by Na decoration of stacking faults in Si solar cells. *Sol. Energy Mater. Sol. Cells* **2013**, *120*, 383–389.
16. Ziebarth, B.; Mrovec, M.; Elsasser, C.; Gumbsch, P. Potential-induced degradation in solar cells: Electronic structure and diffusion mechanism of sodium in stacking faults of silicon. *J. Appl. Phys.* **2014**, *116*, 093510–093517. [[CrossRef](#)]
17. Harvey, S.P.; Aguiar, J.A.; Hacke, P.; Guthrey, H.; Johnston, S.; Al-Jassim, M. Sodium accumulation at potential-induced degradation shunted areas in polycrystalline silicon modules. *IEEE J. Photovolt.* **2016**, *6*, 1440–1445. [[CrossRef](#)]
18. Dong, N.C.; Islam, M.A.; Ishikawa, Y.; Uraoka, Y. The influence of sodium ions decorated micro-cracks on the evolution of potential induced degradation in p-type crystalline silicon solar cells. *Sol. Energy* **2018**, *174*, 1–6. [[CrossRef](#)]
19. Koch, S.; Nieschalk, D.; Berghold, J.; Wendlandt, S.; Krauter, S.; Grunow, P. Potential induced degradation effects on crystalline silicon cells with various antireflective coatings. In Proceedings of the 27th European Photovoltaic Solar Energy Conference and Exhibition, Frankfurt, Germany, 24–28 September 2012; pp. 1985–1990.
20. Mishina, K.; Ogishi, A.; Ueno, K.; Jonai, S.; Ikeno, N.; Saruwatari, T.; Hara, K.; Ogura, A.; Yamazaki, T.; Doi, T.; et al. Plasma-enhanced chemical-vapor deposition of silicon nitride film for high resistance to potential-induced degradation. *Jpn. J. Appl. Phys.* **2015**, *54*. [[CrossRef](#)]

21. Zhou, C.; Zhu, J.; Zhou, S.; Tang, Y.; Foss, S.E.; Haug, H.; Nordseth, O.; Marstein, E.S.; Wang, W. SiO_yN_x/SiN_x stack: A promising surface passivation layer for high-efficiency and potential-induced degradation resistant mc-silicon solar cells. *Prog. Photovolt. Res. Appl.* **2017**, *25*, 23–32. [[CrossRef](#)]
22. Hylsky, J.; Strachala, D.; Hladik, J.; Cudek, P.; Kazda, T.; Vanek, J.; Vyroubal, P.; Stary, J. Design of P-type photovoltaic cells resistant to potential-induced degradation. *IEEE J. Photovolt.* **2018**, *8*, 1215–1221. [[CrossRef](#)]
23. Kapur, J.; Stika, K.M.; Westphal, C.S.; Norwood, J.L.; Hamzavytehrany, B. Prevention of potential-induced degradation with thin ionomer film. *IEEE J. Photovolt.* **2015**, *5*, 219–223. [[CrossRef](#)]
24. Virtuani, A.; Annigoni, E.; Ballif, C. One-type-fits-all-systems: Strategies for preventing potential-induced degradation in crystalline silicon solar photovoltaic modules. *Prog. Photovolt. Res. Appl.* **2019**, *27*, 13–21. [[CrossRef](#)]
25. Hoffmann, S.; Koehl, M. Effect of humidity and temperature on the potential-induced degradation. *Prog. Photovolt. Res. Appl.* **2014**, *22*, 173–179. [[CrossRef](#)]
26. Suzuki, S.; Nishiyama, N.; Yoshino, S.; Ujio, T.; Watanabe, S.; Doi, T.; Masuda, A.; Tanahashi, T. Acceleration of potential-induced degradation by salt-mist preconditioning in crystalline silicon photovoltaic modules. *Jpn. J. Appl. Phys.* **2015**, *54*, KG08–KG12. [[CrossRef](#)]
27. Lausch, D.; Naumann, V.; Breitenstein, O.; Bauer, J.; Graff, A.; Bagdahn, J.; Hagendorf, C. Potential-Induced Degradation (PID): Introduction of a Novel Test Approach and Explanation of Increased Depletion Region Recombination. *IEEE J. Photovolt.* **2014**, *4*, 834–840. [[CrossRef](#)]
28. Pingel, S.; Frank, O.; Winkler, M.; Daryan, S.; Geipel, T.; Hoehne, H.; Berghold, J. Potential induced degradation of solar cells and panels. In Proceedings of the 35th IEEE Photovoltaic Specialists Conference, Honolulu, HI, USA, 20–25 June 2010; pp. 2817–2822.
29. Jaekel, B.; Cosic, M.; Arp, J. Investigation of c-Si modules degradation and recovery effect under high potentials: CV-PID. In Proceedings of the 40th Photovoltaic Specialist Conference, Denver, CO, USA, 8–13 June 2014; pp. 0937–0942.
30. Wang, H.; Cheng, X.; Yang, H.; He, W.; Chen, Z.; Xu, L.; Song, D. Potential-induced degradation: Recombination behavior, temperature coefficients and mismatch losses in crystalline silicon photovoltaic power plant. *Sol. Energy* **2019**, *188*, 258–264. [[CrossRef](#)]
31. Hylsky, J.; Strachala, D.; Vyroubal, P.; Gudek, P.; Vanek, J.; Vanysek, P. Effect of negative potential on the extent of PID degradation in photovoltaic power plant in a real operation mode. *Microelectron. Reliab.* **2018**, *85*, 12–18. [[CrossRef](#)]
32. Yang, H.; Wang, F.; Wang, H.; Chang, J.; Song, D.; Su, C. Performance deterioration of p-type single crystalline silicon solar modules affected by potential induced degradation in photovoltaic power plant. *Microelectron. Reliab.* **2017**, *72*, 18–23. [[CrossRef](#)]
33. Islam, M.A.; Hasanuzzaman, M.; Rahim, N.A. A comparative investigation on in-situ and laboratory standard test of the potential induced degradation of crystalline silicon photovoltaic modules. *Renew. Energy* **2018**, *127*, 102–113. [[CrossRef](#)]
34. Wang, H.; Zhao, P.; Yang, H.; Chang, J.; Song, D.; Sang, S. Performance variation of dark current density-voltage characteristics for PID-affected monocrystalline silicon solar modules from the field. *Microelectron. Reliab.* **2018**, *81*, 320–327. [[CrossRef](#)]
35. Chang, J.; Wang, H.; Yang, H.; Zhang, J.; Huang, J. The Real Situation of Potential-Induced Degradation in Multicrystalline Silicon Photovoltaic Power Plant. In Proceedings of the 43rd IEEE Photovoltaic Specialist Conference, Portland, OR, USA, 5–10 June 2016; pp. 1682–1685.
36. Huang, J.; Li, H.; Sun, Y.; Wang, H.; Yang, H. Investigation on potential-induced degradation in a 50 MWp crystalline silicon photovoltaic power plant. *Int. J. Photoenergy* **2018**, 1–7. [[CrossRef](#)]
37. Masuda, A.; Akitomi, M.; Inoue, M.; Okuwaki, K.; Okugawa, A.; Ueno, K.; Yamazaki, T.; Hara, K. Microscopic aspects of potential-induced degradation phenomena and their recovery process for p-type crystalline Si photovoltaic modules. *Curr. Appl. Phys.* **2016**, *16*, 1659–1665. [[CrossRef](#)]
38. Martinez-Moreno, F.; Figueiredo, G.; Lorenzo, E. In-the-field PID related experiences. *Sol. Energy Mater. Sol. Cells* **2018**, *174*, 485–493. [[CrossRef](#)]
39. Oh, W.; Kim, J.; Kang, B.; Bae, S.; Lee, K.D.; Lee, H.S.; Kim, D.; Chan, S. Evaluation of potential-induced degradation in crystalline Si solar cells using Na fault injection. *Microelectron. Reliab.* **2016**, *64*, 646–649. [[CrossRef](#)]

40. Gou, X.; Li, X.; Yu, J.; Wang, S.; Zhang, X.; Zhou, S.; Fan, W.; Huang, Q. Influence of crystal defect density of silicon wafers on potential-induced degradation (PID) in solar cells and modules. *Phys. Status Solidi A* **2017**, *214*, 1700006. [[CrossRef](#)]
41. Hacke, P.; Spataru, S.; Terwilliger, K.; Perrin, G.; Glick, S.; Kurtz, S.; Wohlgemuth, J. Accelerated testing and modeling of potential-induced degradation as a function of temperature and relative humidity. *IEEE J. Photovolt.* **2015**, *5*, 1549–1553. [[CrossRef](#)]
42. Bauer, J.; Naumann, V.; Grober, S.; Hagendorf, C.; Schutze, M.; Breitenstein, O. On the mechanism of potential-induced degradation in crystalline silicon solar cells. *Phys. Status Solidi–Rapid Res. Lett.* **2012**, *6*, 331–333. [[CrossRef](#)]
43. Masuda, A.; Hara, Y.; Jonai, S. Consideration on Na diffusion and recovery phenomena in potential-induced degradation for crystalline Si photovoltaic modules. *Jpn. J. Appl. Phys.* **2016**, *55*, BF10–BF15. [[CrossRef](#)]
44. Park, J.; Chan, M.K.Y. Mechanism of Na accumulation at extended defects in Si from first-principles. *J. Appl. Phys.* **2018**, *123*. [[CrossRef](#)]
45. Spataru, S.; Hacke, P.; Sera, D.; Packard, C.; Kerekes, T.; Teodorescu, R. Temperature-dependency analysis and correction methods of in situ power-loss estimation for crystalline silicon modules undergoing potential-induced degradation stress testing. *Prog. Photovolt. Res. Appl.* **2015**, *23*, 1536–1549. [[CrossRef](#)]



© 2019 by the authors. Licensee MDPI, Basel, Switzerland. This article is an open access article distributed under the terms and conditions of the Creative Commons Attribution (CC BY) license (<http://creativecommons.org/licenses/by/4.0/>).